An evolutionarily conserved dileucine motif in Shal K+ channels mediates dendritic targeting

Jacqueline F. Rivera[1,3], Shoeb Ahmad[1,3], Michael W. Quick[1–3], Emily R. Liman[1–3] and Don B. Arnold[1–3]

[1] *Program in Molecular Biology,* [2]*Program in Neuroscience and* [3]*Department of Biological Sciences, University of Southern California, 835 W. 37th Street, Los Angeles, California 90089-1340, USA*

Correspondence should be addressed to D.B.A. (darnold@usc.edu)

Published online 18 February 2003; doi:10.1038/nn1020

The molecular mechanisms underlying polarized sorting of proteins in neurons are poorly understood. Here we report the identification of a 16 amino-acid, dileucine-containing motif that mediates dendritic targeting in a variety of neuronal cell types in slices of rat brain. This motif is present in the carboxy (C) termini of Shal-family K+ channels and is highly conserved from *C. elegans* to humans. It is necessary for dendritic targeting of potassium channel Kv4.2 and is sufficient to target the axonally localized channels Kv1.3 and Kv1.4 to the dendrites. It can also mediate dendritic targeting of a non-channel protein, CD8.

The finely tuned electrophysiological properties of neurons depend on precise spatial distributions of ion channels and receptors. The mechanisms by which these distributions are established, maintained and modified in response to physiological stimuli are not well understood. Voltage-gated K^+ channels are ideal models for studying mechanisms of subcellular protein localization because they have a relatively simple and well-understood structure[1] and because the localization patterns of many have been mapped[2]. Moreover, several K^+ channels have a strikingly polarized localization pattern: certain Shaker K^+ channels are localized specifically in the axons of CNS neurons, whereas Shal K^+ channels tend to localize to the somatodendritic compartment[2–7].

At least three different mechanisms may underlie the localization of membrane proteins to specific subcellular compartments in neurons: selective retention, endocytosis and intracellular trafficking. Selective retention is involved in localization of the ion channel dTRP to rhabdomeres and of Kv2.1 to specific regions within the somatodendritic compartment[8,9]. Selective endocytosis is involved in the axonal localization of the sodium channel NaV1.2 through its selective depletion in the somatodendritic area[10]. Selective intracellular targeting of vesicles underlies the localization of the transferrin receptor to the somatodendritic compartment[11].

A key step in further defining mechanisms by which the polarized distribution of a protein can be generated is the identification of signaling motifs within the primary amino-acid (aa) sequence of the protein that specify its subcellular localization[12]. Sequences have been identified in many membrane proteins that are involved in directing the polarized expression of these proteins in epithelial cells[13]. In addition, similarities between basolateral targeting in epithelial cells and dendritic targeting in neurons have been suggested by experiments in which proteins that localize to the basolateral region of epithelial cells localize to the dendritic region when expressed in neurons[14]. Three such proteins—the polyimmunoglobulin receptor, the LDL receptor and the transferrin receptor—are targeted to the basolateral region by short tyrosine-containing motifs[15–18]. Mutation of these motifs results in disruption of somatodendritic targeting after expression of the receptors in neurons[19], although it is not known if they are sufficient to mediate somatodendritic targeting. Motifs associated with dendritic targeting have also been found in ion channels and receptors that are endogenously expressed in neurons. These include regions of 30 amino acids or more in the C termini of the metabotropic glutamate receptors mGluR2 (ref. 20) and mGluR1a (ref. 21) and of the AMPA receptor GluR1(ref. 22). However, there is no evidence that these motifs are conserved in other dendritically targeted membrane proteins.

Here we identify a 16-aa, dileucine-containing motif, conserved in Shal K^+ channels from humans to *C. elegans*, that is both necessary and sufficient to mediate dendritic targeting of membrane proteins in neurons.

Results

Subcellular localization of tagged K+ channels

We chose to study mechanisms of subcellular targeting using the K^+ channels Kv4.2, Kv1.3 and Kv1.4 because of their distinct patterns of localization. Endogenous Kv4.2 is found specifically in the somatodendritic compartment[2,4,6], and Kv1.4 and Kv1.3 are found exclusively in the axonal compartment of CNS neurons[2,4,7]. To facilitate labeling, each channel was tagged by inserting Myc epitopes into extracellular loops (**Fig. 1a**). To confirm that the tagged channels were capable of trafficking to the plasma membrane and forming functional channels, we expressed each in HEK-293 cells and measured K^+ currents in response to voltage steps (**Fig. 1a** and **c**). We also expressed both channel and non-

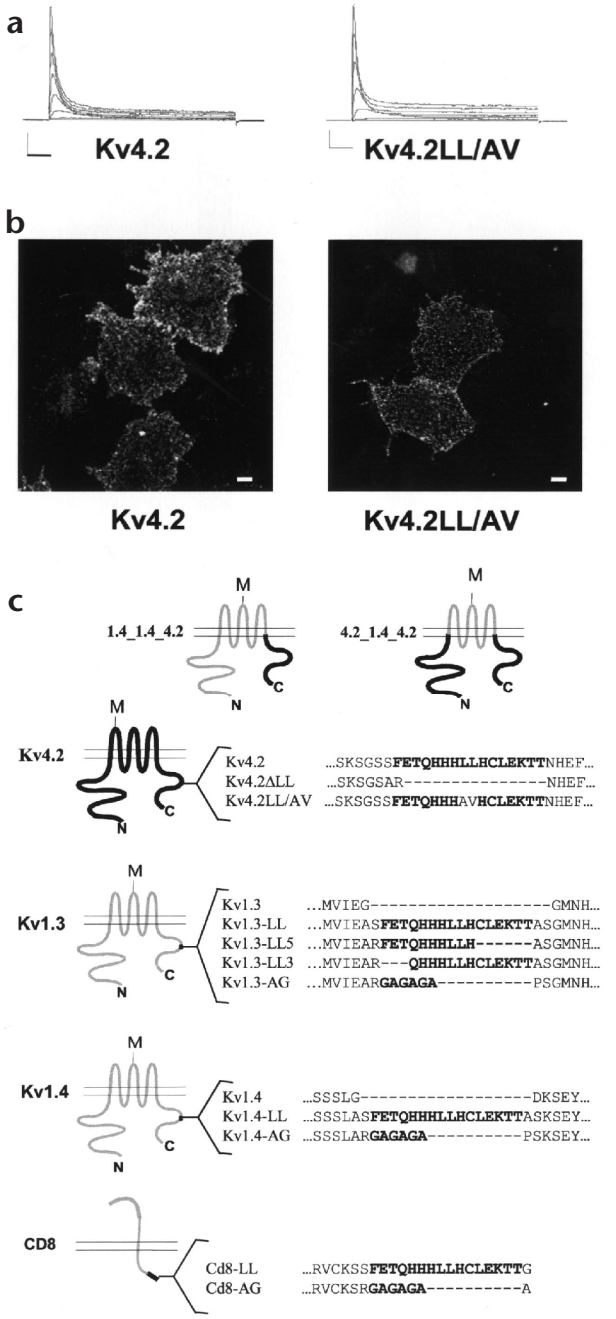

Fig. 1. Characterization of tagged K^+ channel constructs. (**a**) K^+ currents measured with patch-clamp recording from HEK-293 cells transfected with tagged wild-type Kv4.2 and the tagged mutant channel Kv4.2LL/AV. Currents were elicited by voltage steps from a holding potential of –80 mV to between +10 and +60 mV. Scale bar, 500 pA and 50 ms. (**b**) After expression of tagged Kv4.2 and Kv4.2LL/AV in COS-7 cells, anti-Myc surface staining revealed the presence of protein on the cell surface. Scale bar, 10 μm. (**c**) Schematics (not to scale) of K^+ channel and CD8 constructs. In chimeras 1.4_1.4_4.2 and 4.2_1.4_4.2, black represents Kv4.2, and gray represents Kv1.4. M represents the double-Myc tag.

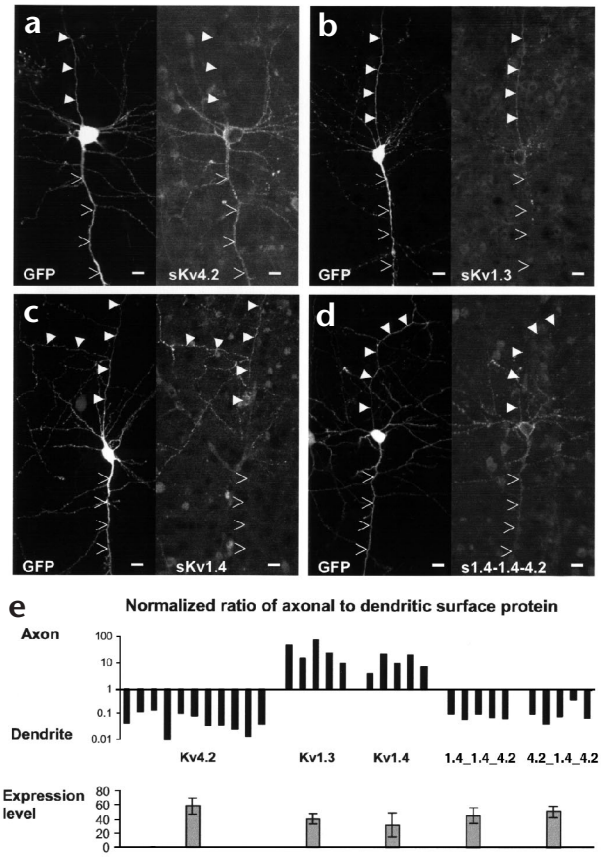

Fig. 2. Subcellular localization of K^+ channel constructs in cortical pyramidal cells in slices. (**a**) GFP and Kv4.2 were coexpressed in a cortical pyramidal cell for 40 h. Anti-Myc surface staining revealed that Kv4.2 was expressed preferentially in the dendrites. (**b**) Surface Kv1.3 localized predominantly to the axon, as did surface Kv1.4 (**c**). (**d**) The chimera 1.4_1.4_4.2 localized preferentially to the dendrites. (**e**) sADR (surface axonal-to-dendrite ratio) is shown for individual cells. Expression levels shown were averaged over all cells that expressed the same construct and are in arbitrary units. Error bars represent standard deviation (s.d.). Filled arrowheads point to the axon; open arrowheads point to the dendrite. Note that the axons in (**c**) and (**d**) have multiple branches and that arrowheads do not point to all minor branches. Scale bars, 10 μm.

channel constructs in COS-7 cells and checked for surface staining with anti-MYC antibodies (**Fig. 1b** and **c**).

Each channel construct was introduced along with green fluorescent protein (GFP) by biolistic transfection into neurons in cultured cortical slices cut from P12–P14 rats[23]. We analyzed the distribution of expressed protein in cortical pyramidal cells, which have clearly identifiable axons and dendrites. We chose initially to look at protein that was expressed on the surface of transfected cells, as an examination of total protein would include protein in intracellular pools and thus possibly confound our results (discussed below). Surface protein was detected by adding primary antibody to live slices, without permeabilization (Methods). The primary antibody was found to penetrate at least 35–40 μm into the slice (data not shown), which was sufficient to stain the dendrites and proximal axons of transfected cells. We confirmed that intracellular protein was not stained using this protocol (see **Supplementary Fig. 1** online).

Expressed, tagged Kv4.2 localized preferentially to the dendrites of pyramidal cells, whereas Kv1.4 and Kv1.3 localized predominantly to axons (**Fig. 2a–c**). Because most proteins that we expressed in this study were present to some degree in the soma, we have described their distributions in terms of axonal protein versus dendritic protein (excluding somatic protein). Accord-

Table 1. Axon-to-dendrite ratios for proteins expressed in cortical pyramidal neurons.

Construct	sADR	tADR
mGFP	1.3 ± 0.5 (*n* = 5)	
Kv4.2	0.06 ± 0.01 (*n* = 11)	0.1 ± 0.02 (*n* = 5)
Kv4.2ΔLL	3 ± 0.8 (*n* = 5)	0.8 ± 0.07 (*n* = 6)
Kv4.2LL/AV	2 ± 0.2 (*n* = 9)	0.9 ± 0.08 (*n* = 5)
CD8	2 ± 0.4 (*n* = 9)	1 ± 0.2 (*n* = 5)
CD8-LL	0.1 ± 0.01 (*n* = 10)	0.02 ± 0.005 (*n* = 5)
CD8-AG	3 ± 0.5 (*n* = 11)	2 ± 0.2 (*n* = 5)
Kv1.3	34 ± 2 (*n* = 5)	9 ± 3 (*n* = 5)
Kv1.3-LL	0.05 ± 0.01 (*n* = 5)	0.2 ± 0.02 (*n* = 5)
Kv1.3-AG	18 ± 2 (*n* = 5)	
Kv1.3-LL5	4 ± 1 (*n* = 5)	
Kv1.3-LL3	9 ± 2 (*n* = 5)	
Kv1.4	13 ± 4 (*n* = 5)	
Kv1.4-LL	0.2 ± 0.04 (*n* = 5)	
Kv1.4-AG	11 ± 3 (*n* = 5)	
1.4_1.4_4.2	0.08 ± 0.01 (*n* = 5)	
4.2_1.4_4.2	0.1 ± 0.05 (*n* = 5)	

ingly, we quantified the degree of localization of expressed proteins as the ratio of the density of surface protein in the axon versus that in the dendrite, a number we refer to as the surface axon-to-dendrite ratio (sADR) (**Supplementary Fig. 2**). A value of one indicates that the protein is present at equal density in the axon and the dendrite; a value greater than one indicates a protein that is localized preferentially to the axon; a value less than one indicates that the protein is localized preferentially to the dendrite. sADR was calculated for at least five different cells for each construct. To verify the reliability of this method, we measured the sADR (Methods) for membrane-associated GFP[24] (mGFP), which is nonspecifically localized, and found it to be 1.3 ± 0.5 (**Table 1**). The average sADR for Kv4.2 was 0.06 ± 0.01, indicating a preferential localization to the dendrite, while those of Kv1.3 and Kv1.4 were 34 ± 12 and 13 ± 4, respectively (**Fig. 2e**). In general, expression levels of different constructs did not vary dramatically. Note that transfected Kv4.2 expressed at a level considerably above that of endogenous Kv4.2 (**Supplementary Fig. 3**), indicating that interactions with endogenous channels probably did not greatly influence the localization of transfected Kv4.2 channels.

Identification of a dendritic targeting motif

To determine regions in the primary structure of the channels that are likely to contain localization motifs, we constructed a series of chimeras by swapping the amino (N) and carboxy (C) termini of Kv1.4 and Kv4.2. Although four of the chimeras were not expressed on the surface of any of the three cell types tested (COS-7, HEK-293 and neurons), the remaining two chimeras provided useful information about the possible location of a dendritic targeting motif. The chimera 1.4_1.4_4.2, which consists of the N terminus and transmembrane region of Kv1.4 and the C terminus of Kv4.2, localized to the dendritic region (**Fig. 2d**). Thus, the replacement of the C terminus of Kv1.4 with that of Kv4.2 caused a dramatic shift from an axonal (sADR, 13 ± 4) to a dendritic localization (sADR, 0.08 ± 0.01). This difference was significant ($P < 0.004$; Wilcoxon-Mann-Whitney test), suggesting the presence of a dendritic targeting signal within the C terminus of Kv4.2. If the C terminus of Kv4.2 contains a dendritic localization signal, then any chimera containing that sequence should localize to the dendritic region. In accord with this, we found that the chimera 4.2_1.4_4.2 also localized to the dendritic region (sADR, 0.1 ± 0.05; $P < 0.004$ compared with Kv4.2).

To identify a dendritic targeting signal within the C terminus of Kv4.2, we searched for motifs conserved among similarly localized Shal channels from different organisms. We found two regions that are conserved between rat Kv4.2 and the somatodendritically localized Shal channel Kv4L from the lobster *P. Interuptus*[5]. The first is found immediately adjacent to the sixth transmembrane domain, suggesting that this region might be important for the gating of the channel rather than sub-

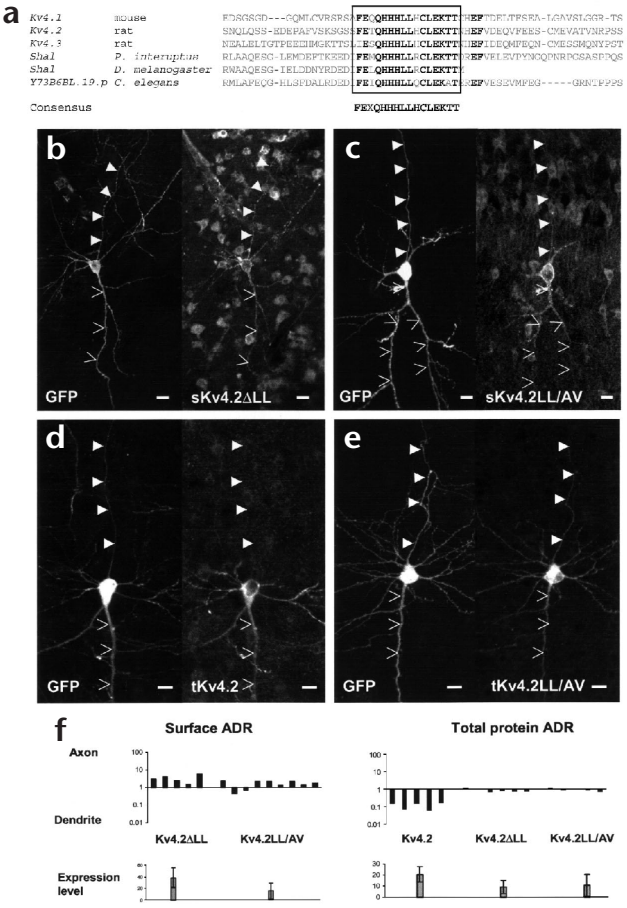

Fig. 3. Alignment of Shal K^+ channels reveals a conserved C-terminal dileucine-containing motif that is necessary for dendritic localization. (**a**) Comparison of the C termini of different Shal K^+ channels. Letters shown in bold are conserved in at least five out of the six sequences. The *C. elegans* gene *Y73B6BL.19.p* is likely a *Shal* gene, as it shares 61% identity with the *P. interuptus Shal* gene. Accession numbers in order: NM_008423, AAB19939, AAC52695, 2207310A, P17971, NM068574. (**b**, **c**) Kv4.2ΔLL and Kv4.2LL/AV localized nonspecifically on the surface of cortical pyramidal neurons. (**d**) Kv4.2 total protein is expressed preferentially in the dendrites. (**e**) Total protein for Kv4.2LL/AV is distributed nonspecifically. (**f**) Comparisons of the ADRs of Kv4.2ΔLL and Kv4.2LL/AV with that of Kv4.2 (**Fig. 2**) show a dramatic shift in localization with the elimination or mutation of the dileucine-containing motif. Expression levels shown were averaged over all cells that expressed the same constructs and are in arbitrary units. Error bars represent s.d. Filled arrowheads point to the axon; open arrowheads point to the dendrite. Scale bars, 10 μm. The prefix 's' (**b**, **c**) refers to surface protein; the prefix 't' (**d**, **e**) refers to total protein.

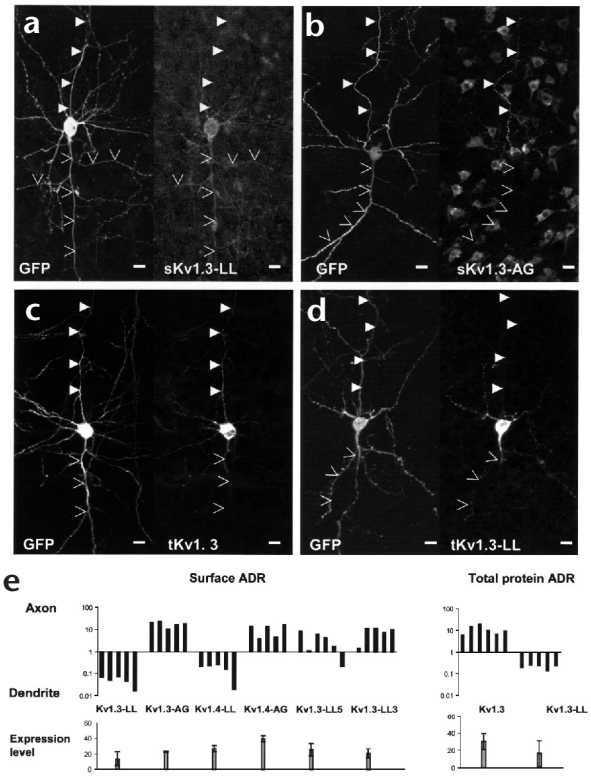

Fig. 4. The dileucine-containing motif is sufficient to mediate dendritic localization in cortical pyramidal neurons. (**a**) Surface Kv1.3-LL localized preferentially to the dendrites. (**b**) Surface Kv1.3-AG localized preferentially to the axon. (**c**) Total Kv1.3 localized preferentially to the axon (**d**) Total Kv1.3-LL localized preferentially to the dendrites. (**e**) ADR calculations verify that addition of the dileucine-containing motif to the axonal channels Kv1.3 and Kv1.4 caused them to localize preferentially to the dendrites over the axon, whereas addition of the AG motif did not affect localization. In addition, deletion of either the 5′ (LL3) or 3′ (LL5) amino acids of the dileucine-containing motif severely impairs its ability to mediate dendritic localization. Total protein ADRs reflect trends that are similar to the surface ADRs. Expression levels shown were averaged over all cells that expressed the same construct and are in arbitrary units. Error bars represent s.d. Filled arrowheads point to the axon; open arrowheads to the dendrite. Scale bars, 10 μm.

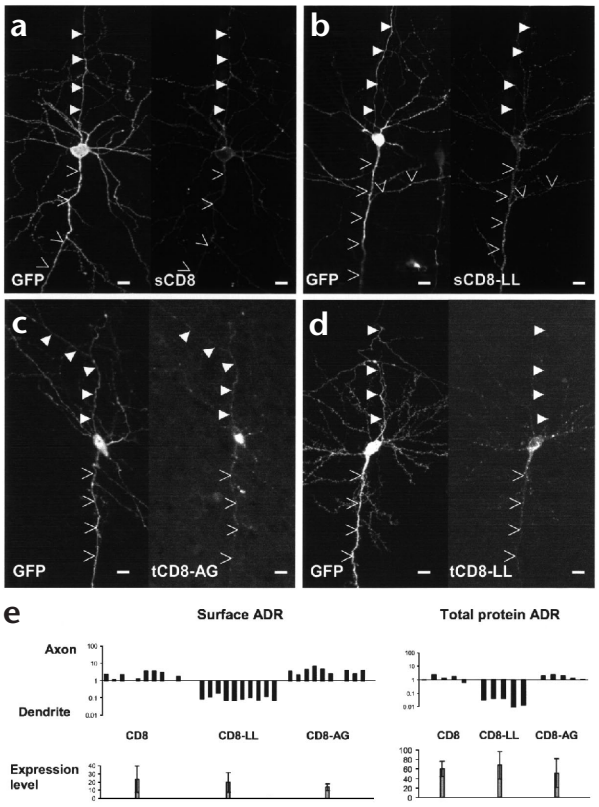

Fig. 5. The dileucine-containing motif mediates dendritic localization of CD8 in cortical pyramidal neurons. (**a**) Surface CD8, identified with an anti-CD8 antibody, localized nonspecifically, although there was bias toward the axon. (**b**) Surface CD8-LL localized preferentially to the dendrites. (**c**) Total CD8-AG localized preferentially to the axon. (**d**) Total CD8-LL localized preferentially to the dendrites. (**e**) ADR calculations confirm that the dileucine-containing motif is sufficient to direct the non-channel protein CD8 preferentially to the dendrites in cortical pyramidal cells. Expression levels shown were averaged over all cells that expressed the same construct and are in arbitrary units. Error bars represent s.d. Filled arrowheads point to the axon; open arrowheads point to the dendrite. Scale bars, 10 μm.

cellular localization[25]. The second is a 16-aa sequence, which spans positions 474–489 of rat Kv4.2, and has 14 amino acids in common with Kv4L. Moreover, additional analysis revealed that 13 of the 16 amino acids are conserved in all known mammalian and invertebrate Shal channels (**Fig. 3a**). In the middle of this motif are two adjacent leucine residues, with a glutamic acid residue positioned six amino acids toward the 5′ end. The motif thus conforms to the $E(X)_{3-5}LL$ configuration of a canonical dileucine-containing motif[26]. Dileucine-containing motifs have been shown to mediate intracellular protein targeting events such as endocytosis in neurons[10] and basolateral targeting in epithelial cells[16], which further suggests that this motif might be involved in dendritic targeting of Kv4.2.

The dileucine motif is necessary for dendritic targeting

To determine whether the dileucine-containing motif at position 474–489 is necessary for dendritic targeting of Kv4.2, we expressed a mutant channel lacking the motif (Kv4.2ΔLL) in cortical slices and then determined its localization. In contrast to the dendritic localization of Kv4.2, Kv4.2ΔLL localized to both the proximal dendrites and the proximal axon (**Fig. 3b**), although it was slightly polarized toward the axon (sADR, 3 ± 0.8) (**Fig. 3f**). In accord with the qualitative differences, the sADRs of Kv4.2 and Kv4.2ΔLL were statistically different ($P < 0.0003$). To determine the functional significance of the two leucines within the dileucine-containing motif, we tested a construct containing alanine and valine in place of the two leucines (Kv4.2LL/AV). Kv4.2LL/AV localized in a nonspecific manner (sADR, 2 ± 0.2) that was similar to the localization pattern of Kv4.2ΔLL (**Fig. 3c** and **f**). The sADR of Kv4.2LL/AV was also statistically different from that of Kv4.2 ($P < 0.0001$). These experiments show that the dileucine motif is necessary for dendritic localization of Kv4.2.

To confirm the results obtained with surface protein, we examined the localization of expressed Kv4.2, Kv4.2ΔLL and Kv4.2LL/AV using permeabilized staining to detect intracellular as well as surface protein. We calculated the total protein axon-to-dendrite ratio (tADR) by determining the ratio of total protein in the axon to that in the dendrite, and normalized by the ratio of the volumes of the two compartments (Methods). Total Kv4.2

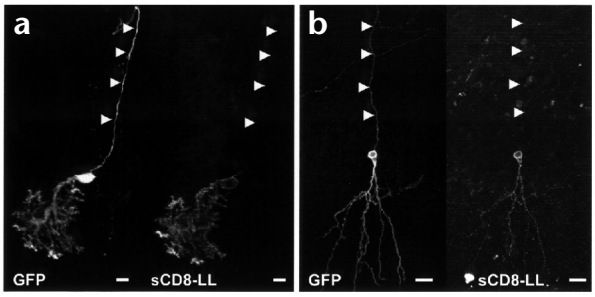

Fig. 6. The dileucine-containing motif functions in multiple cell types. (**a**, **b**) Surface CD8-LL localized preferentially to the dendrites in Purkinje cells of the cerebellum (**a**) and dentate granule cells of the hippocampus (**b**). Filled arrowheads point to the axon. Scale bars, 10 μm. The prefix 's' refers to surface protein.

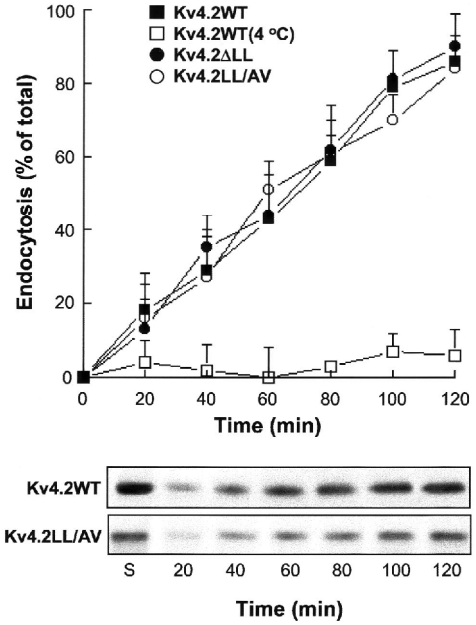

Fig. 7. Mutation of the dileucine-containing motif does not affect the rate of endocytosis. The amount of internalized protein at each time point is plotted as the percentage relative to surface Kv4.2 protein at the start of the assay. Internalization was performed at 24 °C; the non-internalizing control experiment was performed at 4 °C. Data are densitometry measurements from three separate experiments. Representative immunoblots from one experiment are shown for wild-type Kv4.2 (upper blot) and for Kv4.2LL/AV (lower blot). Values under each blot refer to the time permitted for internalization. 'S' denotes the total amount of surface Kv4.2 protein at the start of the assay.

clearly localized predominantly to the dendrites (**Fig. 3d**; tADR, 0.1 ± 0.02), whereas Kv4.2ΔLL (data not shown) and Kv4.2LL/AV (**Fig. 3e**) localized in a nonspecific manner (tADRs, 0.8 ± 0.07 and 0.9 ± 0.08, respectively). The difference in the tADRs for both comparisons was significant ($P < 0.004$). These results confirm those obtained from examination of surface protein. In addition, the fact that very little Kv4.2 protein was detected in the axon indicates that the motif probably works through intracellular trafficking, although roles for the motif in selective docking of vesicles and/or selective endocytosis cannot be ruled out. In this respect, dendritic targeting of Kv4.2 may be similar to that observed for the transferrin receptor[11].

The dileucine motif is sufficient for dendritic targeting

To determine whether the dileucine-containing motif is sufficient to mediate dendritic targeting, it was inserted into the C terminus of the axonally localized channels Kv1.3 and Kv1.4. The resulting channels, Kv1.3-LL and Kv1.4-LL, localized preferentially to the dendritic domain after being expressed in cortical pyramidal cells (sADR, 0.05 ± 0.01 and 0.2 ± 0.04; **Fig. 4a** and **e**) in contrast to the predominantly axonal localization of Kv1.3 and Kv1.4 (**Fig. 2b**, **c** and **e**). The differences between the sADRs of Kv1.3 and Kv1.3-LL and between the sADRs of Kv1.4 and Kv1.4-LL were both significant ($P < 0.004$). Experiments examining total protein that compared localization of Kv1.3 with that of Kv1.3-LL confirmed that addition of the dileucine-containing motif to Kv1.3 caused a dramatic shift from an axonal localization (**Fig. 4c** and **e**; tADR, 9 ± 3) to a dendritic localization (**Fig. 4d** and **e**; tADR, 0.2 ± 0.02) that is statistically significant ($P < 0.002$). These results are consistent with the hypothesis that this motif is both necessary and sufficient for subcellular targeting of the channel. However, an alternative possibility is that insertion of the motif disrupted the signal that mediates axonal targeting in Kv1.3 and Kv1.4. To test this latter possibility, we inserted a tag composed of alanine and glycine residues into the same place into which the dileucine-containing motif was inserted, creating the channels Kv1.3-AG and Kv1.4-AG. Both of these channels localized to the axon (**Fig. 4b** and **e**) and had sADRs (18 ± 2 and 11 ± 3) that were significantly different from those of Kv1.3-LL and Kv1.4-LL, respectively ($P < 0.004$). These results indicate that the change in localization seen following the insertion of the dileucine-containing motif was likely due to the motif itself, rather than to disruption of a signal within Kv1.3 or Kv1.4. Because 13 of the 16 amino acids comprising the dendritic targeting motif are conserved between organisms (**Fig. 3a**), it is likely that more than just the 2 leucine residues are necessary for the motif to function. To test this hypothesis, we tested two constructs containing truncated versions of the dileucine-containing motif in the C terminus of Kv1.3 (**Fig. 1c**). Both Kv1.3-LL5 and Kv1.3-LL3 (**Supplementary Fig. 4** and **Fig. 4e**) were present in both axonal and dendritic processes, although there was a distinct bias toward greater expression in the axon (sADR of Kv1.3-LL5, 4 ± 1; sADR of Kv1.3-LL3, 9 ± 2). These results indicate that although the truncated elements still retained some ability to influence targeting, they were far less efficient than the full-length motif. They are consistent with studies showing that the function of dileucine-containing motifs is critically dependent on the two leucine residues, and that other residues enhance its function[26,27].

To confirm that the motif mediates dendritic targeting in an autonomous manner, we tested whether it could function out of the context of a K^+ channel. We added the motif to the transmembrane protein CD8, which has been found to localize non-specifically[11,19,28]. In our system, CD8 (**Fig. 5a** and **e**) was nonspecifically distributed, with an sADR of 2 ± 0.4, confirming these results. Addition of the dileucine-containing motif to CD8 caused the resulting protein, CD8-LL, to localize to the dendritic region (sADR, 0.1 ± 0.01; **Fig. 5b** and **e**). This was in marked contrast to the localization of CD8-AG, which contains an alanine-glycine motif in place of the dileucine-containing motif, to both the axon and dendrite (sADR, 3 ± 0.5). The sADRs of CD8 and CD8-AG are both significantly different from that of CD8-LL ($P < 0.0001$). These experiments indicate that the dileucine-containing motif is sufficient to direct dendritic localization in

non-channel proteins and that it works in an autonomous manner. We confirmed these results by measuring the localization of total CD8, CD8-AG and CD8-LL. CD8 (data not shown) and CD8-AG (**Fig. 5c**) were found to localize nonspecifically (tADR, 1 ± 0.2 and 2 ± 0.2), whereas CD8-LL was localized to the dendrites (**Fig. 5d** and **e**; tADR, 0.02 ± 0.005). Both differences were significant ($P < 0.004$).

To test whether the motif could function in different cell types, we expressed CD8-LL in Purkinje cells of the cerebellum (**Fig. 6a**) and dentate granule cells of the hippocampus (**Fig. 6b**). In both cases, CD8-LL expressed in the dendrites and was virtually absent from the axon. When CD8-AG was expressed in both cell types, it localized both to the axon and to the dendrite, as in cortical pyramidal cells (data not shown). These experiments indicate that the motif is functional in different neuronal cell types.

One possible mechanism by which dileucine-containing motifs have been shown to effect polarized sorting is through location-restricted endocytosis[10]. Thus, to completely characterize the function of the dileucine-containing motif, we tested whether it could mediate endocytosis. We compared the rate of endocytosis of Kv4.2, Kv4.2ΔLL and Kv4.2LL/AV following expression in COS-7 cells. The rate of endocytosis was not appreciably affected by mutation of the dileucine-containing motif (**Fig. 7**), particularly when compared with the rate of endocytosis at the non-permissive temperature of 4 °C. These results indicate that it is unlikely that the dileucine-containing motif mediates dendritic localization of Kv4.2 through an endocytosis-dependent mechanism.

Discussion

A dendritic targeting motif within Kv4.2

We have identified a 16-aa dileucine-containing motif in the C terminus of K^+ channel Kv4.2 that is necessary and sufficient for dendritic targeting. This motif functions in the context of a heterologous protein and in different neuronal cell types. The motif is present in all Shal K^+ channels and is conserved in evolution from *C. elegans* to humans. These observations suggest that mechanisms of polarized sorting are conserved across different organisms and cell types. The extent to which dendritic targeting motifs homologous to that of Kv4.2 are used by other proteins is unclear. We were unable to find motifs with significant similarity in proteins other than Shal K^+ channels. It is, however, possible that structurally homologous motifs do exist, but do not share sufficient sequence homology to identify them as such. The number of different types of dendritic targeting motifs is also not known. However, evidence that tyrosine-based motifs might be capable of dendritic targeting[19] suggests that more than one type of targeting signal exists.

Combinatorial and default modes of targeting

In addition to identifying a novel dendritic targeting signal, our experiments illuminate the targeting behavior of proteins that contain either more than one signal or no signals. We have shown that addition of the dileucine-containing motif to two axonally localized K^+ channels results in dendritic targeting. Because Kv1.3-LL and Kv1.4-LL contain both axonal and dendritic targeting signals, this result implies that the latter signal is dominant over the former. In this respect, the dendritic signal is similar to the basolateral targeting signal in epithelial cells, which in many cases is dominant over the apical signal[15]. Elimination of the dileucine-containing motif caused Kv4.2 to localize in a nonspecific manner predominantly to the cell body and very proximal dendrites and axon (**Fig. 3a** and **b**). This result implies that the 'default' targeting location for proteins might be the surface of the cell body.

Functional significance of dendritic targeting of Kv4.2

In CA1 hippocampal pyramidal neurons, fast-inactivating K^+ channels such as Kv4.2 block the initiation and propagation of action potentials[29]. Consequently, subcellular targeting of this channel determines which regions of the neuron are capable of initiating and propagating action potentials. The dendritic targeting motif in Kv4.2 positions the channel so that it both restricts action potential initiation to the axonal region and modulates backpropagation of action potentials into the dendrites[30].

Molecular mechanisms of dendritic targeting

Although the molecular interactions between several of the main components of the protein-sorting machinery are known, the mechanisms by which subcellular targeting motifs come to influence the final destinations of proteins in which they are situated are not well understood. Several targeting motifs, such as the canonical dileucine-containing motif, have been shown to bind to subunits of adaptor protein complexes[31,32]. Adaptor proteins, in turn, are necessary for loading proteins into vesicles bound for specific locations within neurons[33]. Vesicles are transported from the trans-Golgi to the plasma membrane by specific kinesin isoforms, which can attach directly to the adaptor proteins[34]. Two possible models of kinesin function suggest alternate mechanisms by which targeting motifs direct subcellular localization. In the first model, each kinesin isoform always travels to the same subcellular region, so the destination of a vesicle (and its contents) is determined by the particular kinesin with which it interacts. In this model, a targeting motif could direct subcellular localization of a vesicle by binding to a particular adaptor protein, which would determine which kinesin isoform transported the vesicle. This model is consistent with the observation that certain kinesins, such as kifC2 (refs. 35,36), kif17 (ref. 37) and kif21b (ref. 38) are found exclusively in the somatodendritic domain. The second model holds that a kinesin is capable of traveling to more than one subcellular location, and its destination is determined by interaction with 'driver' proteins. In such a model, the adaptor protein (and thus the targeting motif) would not necessarily determine which kinesin interacts with a particular vesicle, but would 'steer' the kinesin toward a particular subcellular location either by direct interaction or by interaction through a second or third protein. Evidence for this hypothesis comes from recent observations that interaction with the PDZ domain–containing protein GRIP can cause the kinesin Kif5 to localize to the dendrite[39].

Methods

DNA constructions. Kv4.2, Kv1.3 and Kv1.4 were each labeled with a double-Myc tag inserted after aa residues 221, 315 and 433, respectively. All new restriction sites were generated using PCR mutagenesis with the Quickchange protocol (Stratagene, Cedar Creek, Texas). In Kv1.3–Myc, Asn237 and Asn238 were mutated to Gly and Ser, respectively, to remove glycosylation sites. Kv4.2ΔLL was generated by eliminating aa residues 501–516 of Kv4.2–Myc (**Fig. 1c**). Chimera 1.4_1.4_4.2 consisted of residues 1–561 of Kv1.4 ligated to residues 405–630 of Kv4.2. Chimera 4.2_1.4_4.2 consisted of residues 1–183 of Kv4.2 ligated to residues 308–787 of 1.4_1.4_4.2. Kv4.2LL/AV contains the substitutions L480A and L481V. The tags LL, AG, LL5 and LL3 were each inserted after residue 521 of Kv1.3–Myc to create Kv1.3-LL, Kv1.3-AG, Kv1.3-LL5 and Kv1.3-LL3, respectively. Kv1.4-AG and Kv1.4-LL contain LL and AG tags after residue 607. CD8 constructs were made from *pJPA5–CD8–YFP*[19]. CD8-LL and CD8-AG had their respective motifs inserted after aa residue 218. The last 19 amino acids were truncated from both constructs.

Culturing and transfection. Culturing of slices was as previously described[40]. Slices were cut from the caudal cortex, where Kv4.2 is expressed at low levels[41]. The slices were cultured in medium containing 10% fetal bovine serum (Invitrogen, Carlsbad, California). After incubation for 4 h, the slices were transfected using the Helios gene gun (Biorad, Richmond, California). After transfection, the slices were incubated for an additional 40 h before immunohistochemical analysis. COS-7 and HEK-293 cells were cotransfected with 0.3 μg of the construct to be tested and 0.1 μg of GW-GFP using Effectene reagent and protocol (Qiagen, Valencia, California). All experiments followed the guidelines of the University of Southern California Animal Care and Use Committee and the National Institutes of Health.

Surface protein staining. After incubation for 40 h, the slices were bathed in medium containing 2 μg/ml anti-Myc monoclonal antibody (Covance, Berkeley, California) for 30 min, or 1:50 anti-CD8 mononclonal antibody (Dako, Carpinteria, California) for 5 min, then fixed for 30 min in 2.5% paraformaldehyde and 4% sucrose, permeabilized with 0.2% triton, blocked and incubated in anti-GFP polyclonal antibody (Clontech, Palo Alto, California) at 1:2,000. They were then incubated in 4 μg/ml Alexa 594 goat anti-mouse (Molecular Probes, Eugene, Oregon) and 4 μg/ml Alexa 488 goat anti-rabbit (Molecular Probes) for 1 h. Slices were then cleared with xylene and mounted. COS-7 cells were incubated in primary antibody in medium for 30 min. They were then fixed, permeabilized and incubated in secondary antibody for 1 h, and then mounted onto slides.

Total protein staining. Slices were fixed with 2.5% paraformaldehyde and 4% sucrose for 30 min, followed by permeabilization and incubation with primary antibody for 1 h. Subsequent steps were as above. Comparisons of expressed Kv4.2 with the endogenous channels were performed using the above total protein staining protocol with an anti-Kv4.2 antibody (Sigma, St. Louis, Missouri) at 1:200.

Image capture and analysis. All imaging was done on a Biorad MRC-1024 confocal microscope. Each cell was imaged as a stack of optical sections, 1 μm in depth apart. The cell body was approximately in the center of each image. All calculations were performed on compressed images. For each cell, an initial image of the expressed construct was taken using the 568 nm laser line at the same setting. Additional images were taken of the cell at settings that were more optimal for visualization. Each cell was also imaged using the 488 nm laser line for GFP. Each construct was imaged in at least five different cells (**Table 1**) that were taken from at least three different slices. Cells that had clearly identifiable axons, overall healthy morphology and were not obscured by neighboring cells were chosen on the basis of GFP staining. An axon was identified as a single process that (i) projected in a direction opposite to that of the cortical surface and the apical dendrite and (ii) was clearly longer than any dendrite[40].

To quantify the degree of polarization in the distribution of a particular protein, we defined two ratios, the surface axon-to-dendrite ratio (sADR) and the total protein axon-to-dendrite ratio (tADR). sADR represents the relative density of a particular surface protein in the axon versus that in the dendrite and is defined as follows:

$$\mathrm{sADR} = \frac{F_{\mathrm{P1,\,axon}}}{F_{\mathrm{P1,\,dendrite}}} \Big/ \frac{\mathrm{SA_{axon}}}{\mathrm{SA_{dendrite}}} \qquad (1)$$

where $F_{\mathrm{P1,axon/dendrite}}$ is the relative amount of surface protein P1 in the axon or dendrite and $\mathrm{SA_{axon/dendrite}}$ is the surface area of the axon or dendrite.

We calculated sADR from images obtained using surface staining procedures (**Supplementary Fig. 2**). To calculate the ratio of the surface areas of the two compartments, we assumed that all processes were circular in cross-section. In this case, the ratio of the two surface areas is approximately equal to the ratio of the areas of silhouettes of the two compartments. Note that for a cylinder of radius r and height h, the area of the curved surface is given by $2\pi rh$, which is proportional to the silhouette area, $2rh$.

We defined tADR as follows:

$$\mathrm{tADR} = \frac{\mathrm{tP1_{axon}}}{\mathrm{tP1_{dendrite}}} \Big/ \frac{\mathrm{GFP_{axon}}}{\mathrm{GFP_{dendrite}}} \qquad (2)$$

where $\mathrm{tP1_{axon/dendrite}}$ is the relative amount of the total protein (surface + intracellular) P1 in the axon or dendrite, and $\mathrm{GFP_{axon/dendrite}}$ is the relative amount of GFP in the axon or dendrite. The relative amount of total protein in the axon or dendrite was measured in the same manner as for surface protein.

To test the method for calculating ADR, we expressed *pCA–GAP–GFP*, a membrane-associated GFP (mGFP), and RFP in pyramidal cells. We calculated a simulated sADR by determining the ratio of axonal to dendritic mGFP as if it were a surface-labeled protein. We calculated the ratio of the surface areas of the axon and dendrite using the RFP image (equation 1). Expression levels (in arbitrary units) were calculated by summing the fluorescence in both the axon and the dendrite. Only expression levels of constructs that were detected with the same antibodies (K^+ channels or CD8 constructs) using the same immunocytochemistry procedures can be compared. All measurements were done using ImageJ. All values of ADR were expressed as standard error of the mean (s.e.m.). Comparisons of ADRs were made with the Wilcoxon-Mann-Whitney test. Initial analyses, which were done by unblinded observers, were confirmed for key constructs by a blinded observer.

Endocytosis. Experiments were done in a manner described previously[42], except that internalization was performed at 24 °C.

Electrophysiology. Patch clamp recordings of K^+ currents were obtained from transfected HEK cells using standard methods[43]. Families of current traces were elicited by voltage steps from a holding potential of –80 mV to between +10 and +60 mV.

Note: Supplementary information is available on the Nature Neuroscience website.

Acknowledgments

We thank D. Liu for technical assistance, G. Banker for the CD8 expression construct, K. Moriyoshi for pCA–GAP–GFP and C-P. Ko and S. Bottjer for helpful suggestions on the manuscript. This work was supported by National Institutes of Health grants NS41963 (D.B.A.) and DC04213 (E.R.L.) and a grant from the Whitehall foundation (D.B.A.).

Competing interests statement

The authors declare that they have no competing financial interests.

RECEIVED 26 NOVEMBER 2002; ACCEPTED 16 JANUARY 2003

1. Doyle, D.A. *et al.* The structure of the potassium channel: molecular basis of K^+ conduction and selectivity. *Science* **280**, 69–77 (1998).
2. Veh, R.W. *et al.* Immunohistochemical localization of five members of the Kv1 channel subunits: contrasting subcellular locations and neuron-specific co- localizations in rat brain. *Eur. J. Neurosci.* **7**, 2189–2205 (1995).
3. Smart, S.L. *et al.* Deletion of the K(V)1.1 potassium channel causes epilepsy in mice. *Neuron* **20**, 809–819 (1998).
4. Sheng, M., Tsaur, M.L., Jan, Y.N. & Jan, L.Y. Subcellular segregation of two A-type K^+ channel proteins in rat central neurons. *Neuron* **9**, 271–284 (1992).
5. Baro, D.J. *et al.* Molecular underpinnings of motor pattern generation: differential targeting of shal and shaker in the pyloric motor system. *J. Neurosci.* **20**, 6619–6630 (2000).
6. Song, W.J. *et al.* Somatodendritic depolarization-activated potassium currents in rat neostriatal cholinergic interneurons are predominantly of the A type and attributable to coexpression of Kv4.2 and Kv4.1 subunits. *J. Neurosci.* **18**, 3124–3137 (1998).
7. Cooper, E.C., Milroy, A., Jan, Y.N., Jan, L.Y. & Lowenstein, D.H. Presynaptic localization of Kv1.4-containing A-type potassium channels near excitatory synapses in the hippocampus. *J. Neurosci.* **18**, 965–974 (1998).

8. Tsunoda, S., Sun, Y., Suzuki, E. & Zuker, C. Independent anchoring and assembly mechanisms of INAD signaling complexes in *Drosophila* photoreceptors. *J. Neurosci.* **21**, 150–158 (2001).
9. Lim, S.T., Antonucci, D.E., Scannevin, R.H. & Trimmer, J.S. A novel targeting signal for proximal clustering of the Kv2.1 K+ channel in hippocampal neurons. *Neuron* **25**, 385–397 (2000).
10. Garrido, J.J. *et al.* Identification of an axonal determinant in the C-terminus of the sodium channel Na(v)1.2. *EMBO J.* **20**, 5950–5961 (2001).
11. Burack, M.A., Silverman, M.A. & Banker, G. The role of selective transport in neuronal protein sorting. *Neuron* **26**, 465–472 (2000).
12. Hunziker, W., Harter, C., Matter, K. & Mellman, I. Basolateral sorting in MDCK cells requires a distinct cytoplasmic domain determinant. *Cell* **66**, 907–920 (1991).
13. Matter, K. & Mellman, I. Mechanisms of cell polarity: sorting and transport in epithelial cells. *Curr. Opin. Cell Biol.* **6**, 545–554 (1994).
14. Dotti, C.G. & Simons, K. Polarized sorting of viral glycoproteins to the axon and dendrites of hippocampal neurons in culture. *Cell* **62**, 63–72 (1990).
15. Casanova, J.E., Apodaca, G. & Mostov, K.E. An autonomous signal for basolateral sorting in the cytoplasmic domain of the polymeric immunoglobulin receptor. *Cell* **66**, 65–75 (1991).
16. Matter, K., Yamamoto, E.M. & Mellman, I. Structural requirements and sequence motifs for polarized sorting and endocytosis of LDL and Fc receptors in MDCK cells. *J. Cell Biol.* **126**, 991–1004 (1994).
17. Odorizzi, G. & Trowbridge, I.S. Structural requirements for basolateral sorting of the human transferrin receptor in the biosynthetic and endocytic pathways of Madin-Darby canine kidney cells. *J. Cell Biol.* **137**, 1255–1264 (1997).
18. Kundu, A. & Nayak, D.P. Analysis of the signals for polarized transport of influenza virus (A/WSN/33) neuraminidase and human transferrin receptor, type II transmembrane proteins. *J. Virol.* **68**, 1812–1818 (1994).
19. Jareb, M. & Banker, G. The polarized sorting of membrane proteins expressed in cultured hippocampal neurons using viral vectors. *Neuron* **20**, 855–867 (1998).
20. Stowell, J.N. & Craig, A.M. Axon/dendrite targeting of metabotropic glutamate receptors by their cytoplasmic carboxy-terminal domains [see comments]. *Neuron* **22**, 525–536 (1999).
21. Francesconi, A. & Duvoisin, R.M. Alternative splicing unmasks dendritic and axonal targeting signals in metabotropic glutamate receptor 1. *J. Neurosci.* **22**, 2196–2205 (2002).
22. Ruberti, F. & Dotti, C.G. Involvement of the proximal C terminus of the AMPA receptor subunit GluR1 in dendritic sorting. *J. Neurosci.* **20**, RC78 (2000).
23. Arnold, D., Feng, L., Kim, J. & Heintz, N. A strategy for the analysis of gene expression during neural development. *Proc. Natl. Acad. Sci. USA* **91**, 9970–9974 (1994).
24. Moriyoshi, K., Richards, L.J., Akazawa, C., O'Leary, D.D. & Nakanishi, S. Labeling neural cells using adenoviral gene transfer of membrane-targeted GFP. *Neuron* **16**, 255–260 (1996).
25. Yellen, G. The voltage-gated potassium channels and their relatives. *Nature* **419**, 35–42 (2002).
26. Letourneur, F. & Klausner, R.D. A novel di-leucine motif and a tyrosine-based motif independently mediate lysosomal targeting and endocytosis of CD3 chains. *Cell* **69**, 1143–1157 (1992).
27. Matter, K., Hunziker, W. & Mellman, I. Basolateral sorting of LDL receptor in MDCK cells: the cytoplasmic domain contains two tyrosine-dependent targeting determinants. *Cell* **71**, 741–753 (1992).
28. Craig, A.M., Wyborski, R.J. & Banker, G. Preferential addition of newly synthesized membrane protein at axonal growth cones. *Nature* **375**, 592–594 (1995).
29. Hoffman, D.A., Magee, J.C., Colbert, C.M. & Johnston, D. K^+ channel regulation of signal propagation in dendrites of hippocampal pyramidal neurons. *Nature* **387**, 869–875 (1997).
30. Hoffman, D.A. & Johnston, D. Downregulation of transient K^+ channels in dendrites of hippocampal CA1 pyramidal neurons by activation of PKA and PKC. *J. Neurosci.* **18**, 3521–3528 (1998).
31. Ohno, H. *et al.* Interaction of tyrosine-based sorting signals with clathrin-associated proteins. *Science* **269**, 1872–1875 (1995).
32. Rapoport, I., Chen, Y.C., Cupers, P., Shoelson, S.E. & Kirchhausen, T. Dileucine-based sorting signals bind to the beta chain of AP-1 at a site distinct and regulated differently from the tyrosine-based motif binding site. *EMBO J.* **17**, 2148–2155 (1998).
33. Dwyer, N.D., Adler, C.E., Crump, J.G., L'Etoile, N.D. & Bargmann, C.I. Polarized dendritic transport and the AP-1 mu1 clathrin adaptor UNC-101 localize odorant receptors to olfactory cilia. *Neuron* **31**, 277–287 (2001).
34. Nakagawa, T. *et al.* A novel motor, KIF13A, transports mannose-6-phosphate receptor to plasma membrane through direct interaction with AP-1 complex. *Cell* **103**, 569–581 (2000).
35. Hanlon, D.W., Yang, Z. & Goldstein, L.S. Characterization of KIFC2, a neuronal kinesin superfamily member in mouse. *Neuron* **18**, 439–451 (1997).
36. Saito, N. *et al.* KIFC2 is a novel neuron-specific C-terminal type kinesin superfamily motor for dendritic transport of multivesicular body-like organelles. *Neuron* **18**, 425–438 (1997).
37. Setou, M., Nakagawa, T., Seog, D.H. & Hirokawa, N. Kinesin superfamily motor protein KIF17 and mLin-10 in NMDA receptor-containing vesicle transport. *Science* **288**, 1796–1802 (2000).
38. Marszalek, J.R., Weiner, J.A., Farlow, S.J., Chun, J. & Goldstein, L.S. Novel dendritic kinesin sorting identified by different process targeting of two related kinesins: KIF21A and KIF21B. *J. Cell Biol.* **145**, 469–479 (1999).
39. Setou, M. *et al.* Glutamate-receptor-interacting protein GRIP1 directly steers kinesin to dendrites. *Nature* **417**, 83–87 (2002).
40. Arnold, D.B. & Clapham, D.E. Molecular determinants for subcellular localization of PSD-95 with an interacting K^+ channel. *Neuron* **23**, 149–157 (1999).
41. Serodio, P. & Rudy, B. Differential expression of Kv4 K^+ channel subunits mediating subthreshold transient K^+ (A-type) currents in rat brain. *J. Neurophysiol.* **79**, 1081–1091 (1998).
42. Whitworth, T.L. & Quick, M.W. Substrate-induced regulation of gamma-aminobutyric acid transporter trafficking requires tyrosine phosphorylation. *J. Biol. Chem.* **276**, 42932–42937 (2001).
43. Koren, G., Liman, E.R., Logothetis, D.E., Nadal-Ginard, B. & Hess, P. Gating mechanism of a cloned potassium channel expressed in frog oocytes and mammalian cells. *Neuron* **4**, 39–51 (1990).

An evolutionarily conserved dileucine motif in Shal K^+ channels mediates dendritic targeting

Jacqueline F. Rivera, Shoeb Ahmad, Michael W. Quick, Emily R. Liman, Don B. Arnold
Nat. Neurosci. **6, 243–250 (2003).**

In the Materials and Methods section, the authors stated incorrectly that Kv4.2 contains a double-MYC tag. Kv4.2 and mutant Kv4.2 constructs contain 8 tandem MYC tags.

Speed of visual processing increases with eccentricity

Marisa Carrasco, Brian McElree, Kristina Denisova & Anna Marie Giordano
Nat. Neurosci. **6, 699–670 (2003).**

The word "increasing" was written when "decreasing" was intended on page 2, left column, 2nd paragraph, lines 1 and 2. The sentence should read: "These results provide the first behavioral evidence that either decreasing eccentricity or stimulating..."